5.4 NEARSHORE WAVE AND CURRENT MEASUREMENTS/PREDICTIONS ON THE TEXAS COAST

Philippe E. Tissot, Larry Dell, James Rizzo & Deidre Williams
Conrad Blucher Institute, Texas A&M University-Corpus Christi, Corpus Christi, Texas

1. INTRODUCTION

The movement of water along the coastline of the Gulf of Mexico is affected by local tide, atmospheric forcings and by larger circulation patterns. Measurement and modelling of deep water ocean currents in the Gulf is well documented (e.g. Sturges and Lugo-Fernández, 2005). In the Northwest Gulf of Mexico near real-time measurements of offshore currents along the continental shelf are provided by the Texas Automated Buoy System (TABS) (Guinasso et al., 2009) and wave and atmospheric conditions are available thanks to several buoys from the National Data Buoy Center (NDBC 2015). Water levels and atmospheric conditions are continuously monitored by stations of the Texas Coastal Ocean Observation Network (Rizzo et al. 2014). However at present there is only one permanent station in the Gulf of Mexico that measures water level in the nearshore region along the Texas coast. Several other stations measure water level but are protected by ship channel jetties. There are presently no permanent stations measuring nearshore ocean currents or wave climate along the Texas open coast. A better record and understanding of these conditions are important for a number of applications including oil spill preparation and response as well as the maintenance and design of coastal infrastructure.

Two current profilers were installed during spring 2014 on Bob Hall Pier near Corpus Christi, Texas. The pier is located on North Padre Island near two inlets and close to sensitive avaian and aquatic habitat. The sensors provide near real-time measurement of nearshore conditions including significant wave height, typical wave period, average along and cross shore currents as well as horizontal current profiles for both sensors. In addition to providing observations in a variety of conditions, the sensors provide near real-time information. The resulting data suite is applicable to oil spill planning and response, search and rescue situations, reporting surf conditions, and alerting beach-goers to conditions favorable to the onset of rip currents. The measurements may also be applied to model sediment transport in support of local beach nourishment operations at a nearby popular beach located along North Padre Island.

* *Corresponding author address*: Philippe E. Tissot, Texas A&M University-Corpus Christi, Conrad Blucher Institute, 6300 Ocean Drive, Corpus Christi, TX 78412; e-mail: philippe.tissot@tamucc.edu.

The information shared in this extended abstract provides; details of the experimental set-up, a summary of initial observations, comparison of the measurements with other nearby more permanent atmospheric and oceanic time series, and output from a NOAA operational model. Finally, two simple nowcasting models based on inputs from other near-real time sensors and their performance are presented. Depending on applications and accuracy such models could estimate the presently measured nearshore conditions once the equipment is removed.

2. EXPERIMENTAL SET-UP

Measuring currents in the nearshore environment can be challenging due to the inherently rough sea state, sediment transport, submerged obstructions, and interference by manmade structures such as jetties, groins, or inlets. The project took advantage of a 378 m long pier located along a portion of the coast known as the Coastal Bend (Figure 1).

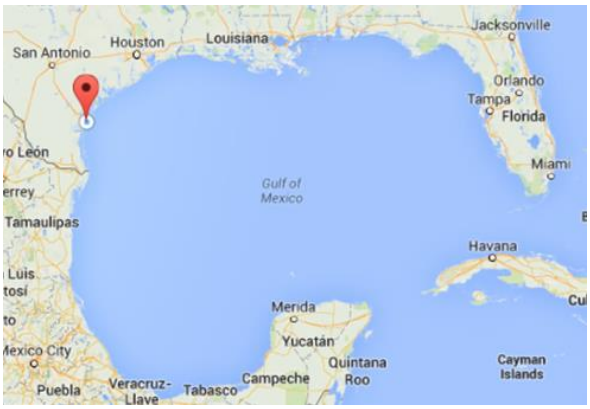

Figure 1. Location of the experiment along the shores of the Coastal Bend in the northwestern part of the Gulf of Mexico.

Two 2D current profilers, both Xylem (Sontek/YSI) Argonaut SL500 (500 kHz), were selected, in part, for their range, form factor, narrow beams and experience of the team in deployment and maintainence of these sensors (Sontek 2009). The sensors are bolted to stainless steel carts movable along I-Beams allowing for easy access and positioning of the sensors. One of the sensors, labeled as “offshore looking sensor”, is attached to an I-Beam secured to the south pile of the platform located next to the offshore end of the pier (see Figures 2 and 3). The platform houses a permanent

NOAA National Water Level Observing Network or NWLON (NOAA 2015) station measuring and recording water level and meteorological conditions. The collocation of the current profilers and the NWLON Corpus Christi station provides for a more comprehensive data suite that may be applied to both local analysis and more extensive large-scale modeling opportunities. The second current profiler, labeled as "nearshore looking sensor", is attached to a pier pile approximately 30 m shoreward from the offshore looking sensor.

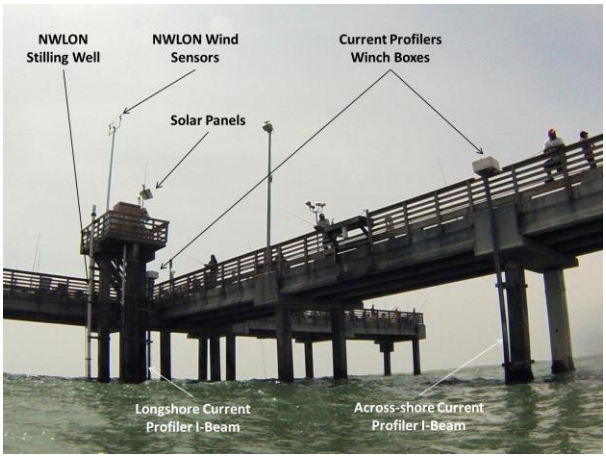

Figure 2. Illustration of the overall experimental geometry with the locations of both the offshore and the nearshore looking current profilers at the seaward end of Bob Hall pier.

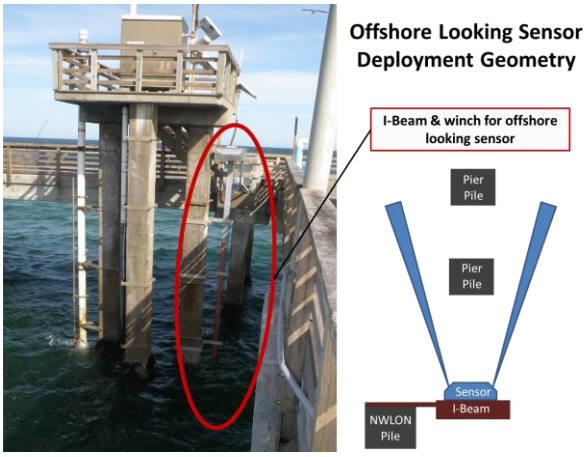

Figure 3. Illustration of the experimental geometry for the offshore looking sensor secured to a pile of the structure housing the Corpus Christi NWLON station.

The offshore looking sensor is set up to provide current profiles from 10 to 120 m offshore from the sensor in bins of 11 m. The sensor also measures 1024 s time series pressure data leading to the computation of significant wave height and typical wave period. Measurements from the offshore looking sensor are recorded at a 30-min interval. The nearshore looking sensor measures current in narrower bins of 5 m starting 1.5 m away from the instrument and up to 51 m in a direction parallel to the shoreline. Measurements of the nearshore looking sensor are recorded at a 6-min interval. The locations and approximate range of the current profilers are illustrated in Figure 4.

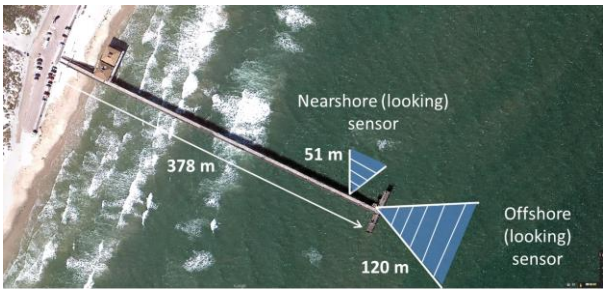

Figure 4. Illustration of the experimental geometry with the locations of the current profilers on the pier and the approximate volumes sampled by each divided in ten bins.

The exact location of the two sensors and their supporting infrastructure was selected to minimize interaction with fishermen who regularly utilize the pier. In particular, the offshore looking sensor was not mounted to one of the most seaward piles of the pier as these locations are frequently occupied by fishermen. Instead the offshore looking sensor was mounted to the NWLON platform located just behind the T-head of the pier limiting interferences with pier users. The set-up includes sound beams passing in between the nearby pier piles as illustrated in Figure 3. While the two sound beams are sufficiently narrow to avoid interferences by the piles, additional side lobe energy (Sontek 2009) can potentially interfere with the nearby piles and affect measurements. Based on sensor beam diagnostics and the analysis of the standard error associated with each current bin (see section 3), it was determined that the proximity of the pier piles has no impact on the measurements past 21 m away from the sensor.

3. OBSERVATIONS

3.1 Range of Consistent Current Measurements

As described in the previous section both sensors measure current profiles within 10 bins. While the offshore looking sensor is set up for a maximum range of 120 m, water conditions, e.g. the amount of particulates in the water (Sontek 2009), will impact the strength of the reflected signal and therefore the actual useful range of measurements. The horizontal profiles or the series of measurements for each of the 10 bins for the signal to noise ratio (Figure 5) and the standard error (Figure 6) are considered to determine the range of consistent current measurements.

The median signal to noise ratio decreases progressively after the first bin. The distributions are

symmetric up to and including bin 6 coinciding with a distance of 76 m. The signal to noise ratios for bins further offshore have a large portion of small numbers. The large number of outliers for bins 7 through 10 indicates that under some conditions the signal to noise ratio for these bins can be sufficient to potentially yield useful information.

The distributions of the standard errors of the current measurements in Figure 6 are relatively stable with the upper bound of the boxplot staying below 0.01 m/s up to bin 5. Starting with bin 6, the medians and upper bounds of the boxplots increase rapidly. Based on this analysis, current measurements are considered consistent up to bin 5 or a distance of 65 m.

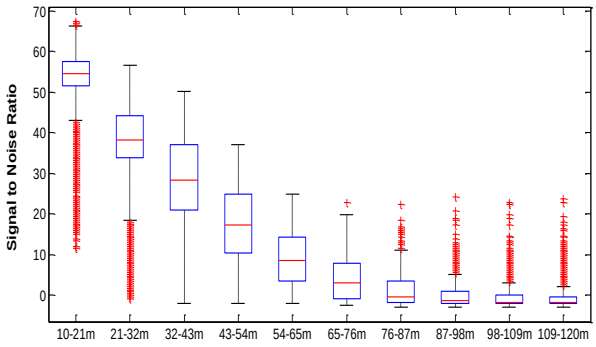

Figure 5. Change in the signal to noise ratio along the measurement range of the offshore looking sensor.

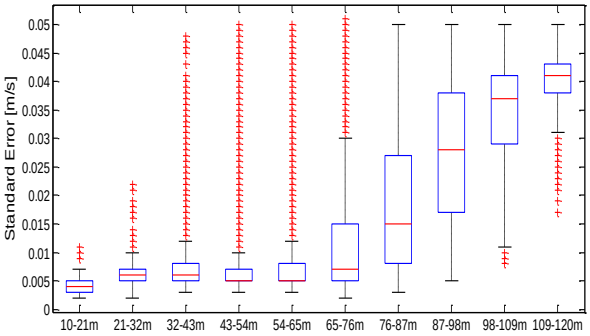

Figure 6. Change in the standard error along the measurement range of the offshore looking sensor.

The measurement consistency at the short end of the current profiles was further assessed by considering in Figure 7 the absolute value of the longshore current profile distributions up to 65 m or bin 5. The distribution of the first bin clearly indicates slower currents as compared to the bins further away from the sensor. The slower currents are, in part, due to the influence of the pier adjacent to this bin and may also be related to the presence of a large migrating sand bar that was identified immediately in front of the pier during installation. However, the possible influence of interferences between the sensor sound beam side lobes and pier piles could also be affecting the measurements and therefore measurements in bin 1 have so far been discounted. Accordingly, bins 2 through 5 are considered reliable for the analysis of longshore currents under the present configuration. Time series of longshore currents measured in each of the four bins are compared in Figure 8 showing these measurements to be largely equivalent.

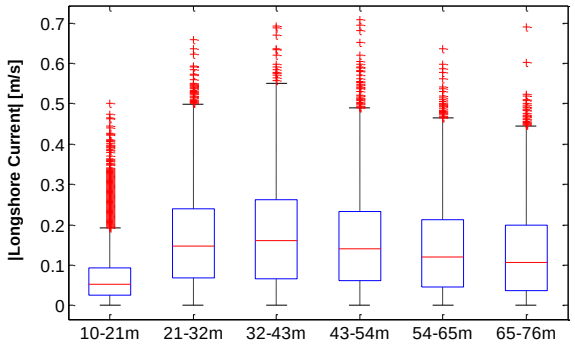

Figure 7. Current distributions for the first six bins.

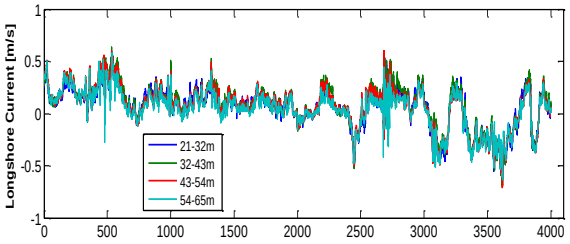

Figure 8. Comparison of the current time series measured for bins 2 through bin 5 showing the consistency of the measurements for these four bins.

For the nearshore looking sensor the maximum range of the profile is set at 51 m, a distance too short to be affected by the strength of the signal at that location. Also, there are no limitations on short range measurements as there are no structures in front of the sensor. As the nearshore waters are shallower, limitations for this sensor are associated with large waves and possibly migrating sand bars. The vertical span of the sound beams at the end of the measurement range (51 m) is 3.4 m for the SL 500 and is well contained within the water column, about 5.5 m deep at that location. During large wave events the depth of the water column is reduced leading to interferences with the air water interface at the end of the measurement range, first for the shoreward beam. Cross shore currents should be small, substantially below 1 m/s, except during special events such as the onset of rip currents or interferences. Figure 9 illustrates across-shore current measurements for bins 1 (1.5-6.5 m), 5 (21.5-26.5 m), and 10 (46.5-51.5 m) between June 10th and September 25th 2014. The largest wave event with significant wave heights up to 1.6 m took place on September 3rd during the landfall of Tropical Storm Dolly south of the Texas/Mexico border. Cross shore currents

in bin 10 alternate between large positive and negative values likely resulting from the repeated interference with the air-sea boundary. Positive or offshore currents larger than 1 m/s would be consistent with the onset of rip currents if not followed by very large negative or onshore currents. Fluctuations between large onshore and offshore cross-shore currents are clearly observed for bins 8, 9 and 10 during the landing of tropical storm Dolly. Smaller wave events also resulted in higher than normal yet much smaller offshore currents, < 0.5 m/s. However, during these events only higher offshore currents were observed; these strong offshore currents were not followed by high onshore currents during these events making it unlikely that interferences with the air-sea surface affected these measurements. The authors have yet to unambiguously identify the presence of rip currents in the experiment cross shore current profiles.

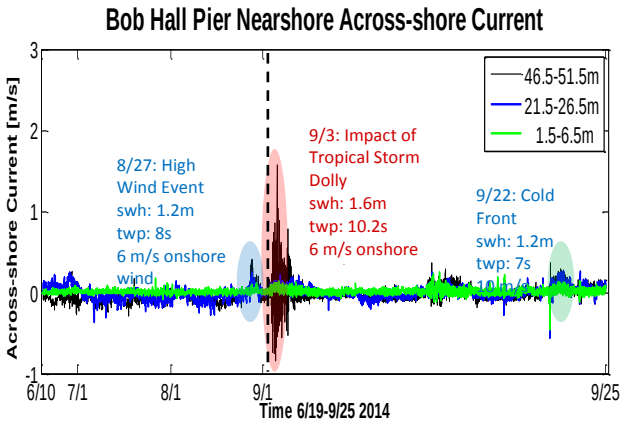

Figure 9. Time series of alongshore and cross-shore wind measurements at the co-located NWLON station during the study period.

3.2 General Conditions and Observations

Coastal hydrodynamics along the south Texas coast is influenced by one of the windiest coastal climates in the United States combined with small tidal ranges. Wind distributions are therefore essential to the analysis of longshore currents. Wind measured at the collocated NWLON station is used for this study. The wind signal is first split between alongshore and cross-shore directions. Time series of both wind components during the study are presented in Figure 10 and a wind rose for the same measurements is presented in Figure 11. Figure 10 illustrates a predominantly strong onshore flow and variable alongshore winds most of the year. S tronger northerly winds accompany the passage of cold fronts starting in September. The wind rose in Figure 11 further indicates the predominance of southeasterly winds with occasional interruption by pulses of strong northerly flow.

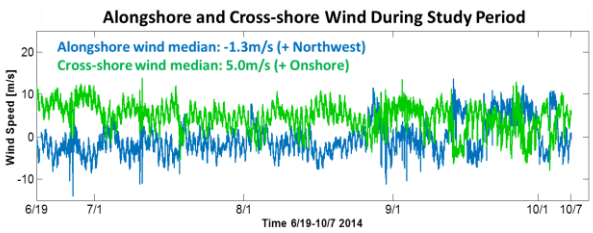

Figure 10. Time series of alongshore and cross-shore wind measurements at the co-located NWLON station during the study period.

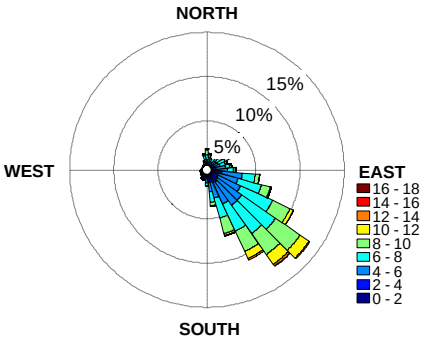

Figure 11. Wind rose for winds during the study period.

Table 1 presents statistical summaries of the longshore current and wave measurements during the study period. The longest typical wave period of 11.2 s was observed during the influence of Tropical Storm Dolly as well as the largest significant wave height of 1.8 m. Longshore currents were summarized using the 5th bin of each sensor. Both sensors measured longshore currents within the range of -0.6 and +0.6 m/s, with similar median longshore currents.

Table 1. Summary of wave and longshore current measurements during the observation period (6/9-10/11, 2014).

	Median	Range
Wave Measurements		
Significant Wave Height	0.7 m	[0.1m, 1.8 m]
Typical Wave Period	5.5 s	[2.1 s, 11.2 s]
Current Measurements		
Nearshore Longshore Current	0.04 m/s	[-0.6 m/s, 0.6 m/s]
Offshore Longshore Current	0.07 m/s	[-0.6 m/s, 0.6 m/s]

The wave height distribution during the study period is illustrated in Figure 12. The longshore currents measured by the two sensors are further compared in Figure 13. The currents measured by the nearshore looking sensor are landward of the last sandbar while

the currents measured by the offshore looking sensor are offshore of the last sand bar with the median of one bin about 90 m further offshore from the comparative bin. While the ranges of the longshore current measurements of the two sensors are the same, differences can be observed particularly during the influence of Tropical Storm Dolly when the nearshore longshore current became substantially larger than the longshore currents measured by the offshore looking sensor. Other differences in the longshore current are well defined during the passage of two cold fronts.

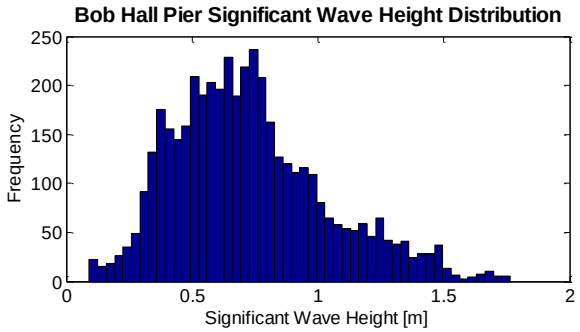

Figure 12. Significant wave height distribution during the study period.

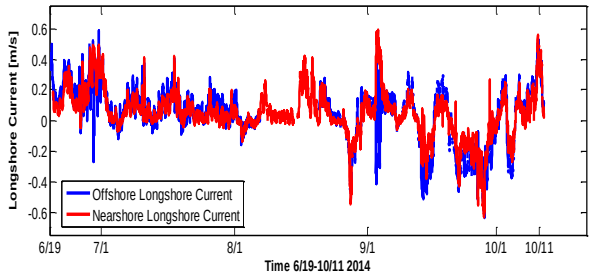

Figure 13. Comparison of longshore currents measured by the offshore looking sensor (behind the last bar) and the nearshore looking sensor (landward of the last bar).

To conclude this preliminary analysis, several correlation coefficients were computed to quantify the relative importance of wind and other forcings on the longshore currents at the study location. The correlations of longshore currents with along shore wind are respectively:

Nearshore longshore current = 0.73
Offshore longshore current = 0.87

The correlations of longshore currents with significant wave heights are respectively:

Nearshore longshore current = 0.22
Offshore longshore current = 0.03

Other significant correlations include:

Significant wave height and across shore currents (nearshore = 0.28, offshore = 0.14)

Cross-shore wind & significant wave height = 0.26

The correlation between along shore winds and the alongshore currents measured seaward of the pier is particularly strong at 0.87 leading to the possibility of nowcasting local longshore current based on local wind measurements. The longshore current measured from the more landward sensor is smaller at 0.73. The correlations with significant wave height are significant and larger for the nearshore longshore current indicating that wave action is likely the cause of the differences in the correlations between along shore wind and the two alongshore currents.

4. COMPARISON WITH OFFSHORE CURRENTS

The longshore currents are compared in this section with currents measured further offshore by TABS buoy D. The location of TABS Buoy D, the closest buoy to the project site, is illustrated in Figure 14. A comparison of the longshore currents is presented in Figure 15. The longshore currents are generally similar at both locations as illustrated in the figure and quantified by a strong correlation coefficient of 0.69. The largest difference is observed during the influence of Tropical Storm Dolly with longshore currents directed downcoast at TABS Buoy D but upcoast at the project location.

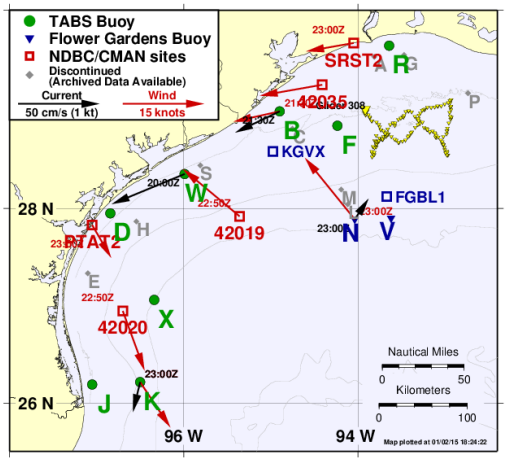

Figure 14. Map with the locations of the TABS Buoys (TABS 2015).

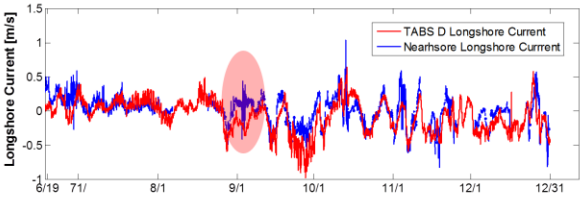

Figure 15. Comparison of nearshore (Bob Hall Pier) and offshore (TABS D) longshore currents during the project period including emphasis on periods of divergences.

5. NOWCASTING OF WAVE HEIGHTS

Wave heights can also be estimated based on the standard deviation of the water levels if measured at a nearby location (Parker 1991 and Park and al. 2014). For this study water levels are measured at the collocated Corpus Christi NWLON station making it another ideal test case. The modeling approach is to fit a linear regression based on the two time series. A scatter plot illustrates the process in Figure 16.

For this particular case the linear regression model is expressed as follows:

Significant Wave Height ~= 6.519 x standard deviation (water levels) + 0.1114.

Model residuals are presented in Figure 17 showing relatively little bias and with standard deviation of 0.15 m. Model performance will be improved by considering only wave heights above a threshold and including more data presently being collected.

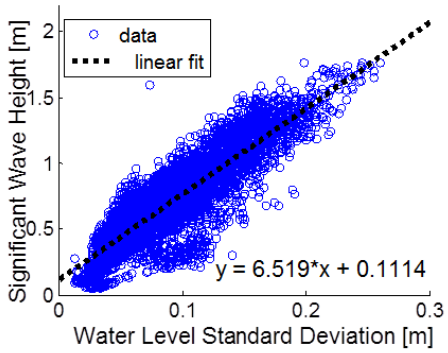

Figure 16. Scatter plot of significant wave heights vs water level standard deviation with illustration of the linear regression.

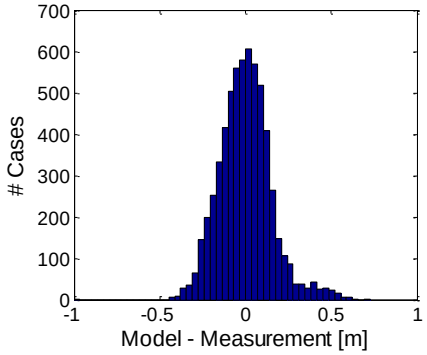

Figure 17. Residual for the significant wave height model during the study period.

6. NOWCASTING OF LONGSHORE CURRENTS

Based on the strong correlation between the alongshore wind and the longshore current, a nowcasting model was calibrated. A neural network approach was selected based on past successes to predict operationally water levels (Cox et al. 2002, Tissot et al. 2003, Tissot et al. 2004) and water temperatures (Simionello et al.2010). Neural networks can be considered as universal approximators with the ability to model nonlinear processes without a priori assumptions of functionality between predictors and predictand. Neural Networks are well suited for nowcasting implementations as once trained computations are virtually instantaneous for a system ingesting near real-time data. The model used for this work is illustrated in Figure 18 and is calibrated and evaluated using the Matlab computational environment (Matlab 2014). For each model calibration, the experimental data set is randomly split between a training (65%), a validation (15%) and a testing (20%) set for each trial. Model training is performed using the Levenberg Marquardt algorithm as implemented in Matlab. Models with 5 hidden neurons were selected after testing models with the number of hidden neurons varied between 1 and 10.

Results are presented in Table 2. A neural network model applying only the input of measured alongshore wind at the same location results in a rmse of 0.1 m/s which is already a useful nowcast. Adding a secondary input of measured offshore longshore currents at the TABS D buoy decreases the rmse by 0.005 m/s. A more substantial improvement is obtained with a rmse of 0.074 m/s when adding significant wave height as an input. As significant wave height is measured by the current profiler, an operational nowcast will have to use the standard deviation of water levels once the sensor is removed. The rmse of the neural network increases a bit from 0.074 m/s to 0.080 m/s after switching the third input from significant wave height to the standard deviation of water levels.

Table 2. Performance of the neural networks trained to nowcast longshore current (bin 5 currents measured by the offshore looking sensor) at the study location.

Input(s)	Mean RMSE [m/s]	RMSE Standard Deviation Over 10 Trials
Alongshore Wind Only	0.100	0.003
Alongshore Wind + Offshore Longshore Current	0.095	0.002
Alongshore Wind + Offshore Longshore Current + Significant Wave Height	0.074	0.003
Alongshore Wind + Offshore Longshore Current + Standard Deviation of Water Levels	0.080	0.002

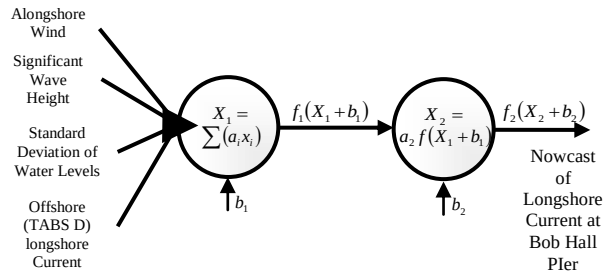

Figure 18. Illustration of a neural network trained to predict longshore currents based on wind measurements including inputs considered.

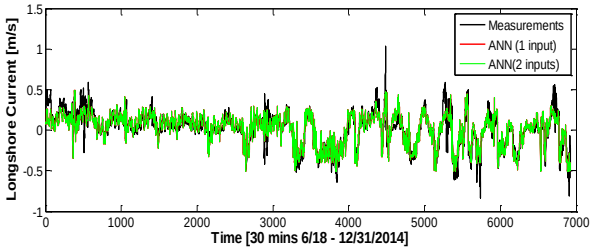

Figure 19. Comparison of measured and nowcasted longshore currents.

7. COMPARISON WITH NOAA NGOFS CURRENT NOWCASTS

NOAA recently made publicly available predictions from the Northern Gulf of Mexico Operational Forecast System or NGOFS (Wei et al. 2014), a 3D numerical hydrodynamic model providing predictions for multiple meteorological and oceanographic variables. Grid resolution ranges from 10 km to 600 m, with the smallest resolution near the coast. As part of the model discussion and documentation (Wei et al. 2014) performance was assessed based on four parameters: water level, current velocity, temperature and salinity measured at 72 stationary stations within the model grid. A number of the stations are along the Gulf of Mexico shorelines however currents are only measured for inland bays and estuaries. The stations of the TABS buoy network (TABS 2015) provide current verification for further offshore locations. In particular near surface currents are assessed for buoys B, W, D, and J deployed in average depths of about 20 m. However no assessment was so far possible for predictions along the open coast.

Figure 20 illustrates the resolution of the NGOFS model around the project station and the relative position of Bob Hall Pier within NGOFS element # 50649. An initial comparison was conducted for 58 initial state of the water current forecast, or time zero predictions, between October 1, 2014 and February 6, 2015. This preliminary comparison does not show a significant bias at 0.005 m/s and yields a root mean square error of 0.117 m/s. The comparison will be extended to a more extensive data set.

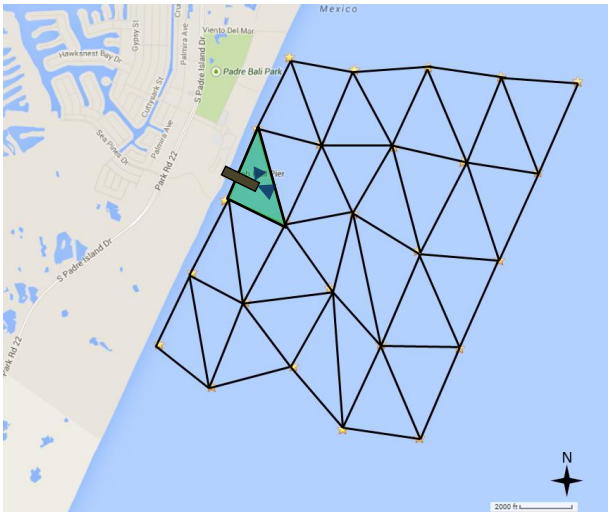

Figure 20. Location of the NGOFS grid element (element # 50649) corresponding to the project sensor location on Bob Hall Pier, Texas.

8. ACCESS TO DATA

Project data can be accessed through the Conrad Blucher Institute website at the following station webpages:

Offshore looking sensor:
http://www.cbi.tamucc.edu/obs/260

Nearshore looking sensor:
http://www.cbi.tamucc.edu/obs/259

For the offshore looking sensor, Velocity X displays the longshore current with a positive current indicating a south-southeast direction. Velocity Y corresponds to the cross shore current with a positive current indicating an offshore direction.

For the nearshore looking sensor, Velocity X corresponds to the crossshore current with positive values indicating an offshore current. Velocity Y with positive values indicates a longshore current in the North-Northwest direction.
Wave and longshore current measurements are also accessible through a website formatted for smartphone users. The page (see Figure 21) is accessible at http://cbi-apps.tamucc.edu/bhpwave/ and also provides the latest atmospheric conditions and other measurements such as water level and water temperature at the collocated NWLON station.

Figure 21. Example of display of conditions with the website optimized for smartphone display at the sensors location.

9. DISCUSSION & CONCLUSIONS

Two current profilers and wave sensors were installed during spring 2014 on a pier located on the open coast near Corpus Christi, Texas. One of the sensors is oriented to monitor conditions offshore of the pier while the other sensor is positioned to measure profiles in a direction parallel to the shoreline. Measurements during the second part of 2014 yielded significant wave heights ranging from 0.1 to 1.8 m and typical wave periods between 2.1 and 11.2 s. Longshore currents measured by both sensors, one offshore of the last sand bar and the other typically inside of this last bar, were both in a range -0.6 to 0.6 m/s. The strongest currents, the largest significant waves and the longest typical wave periods were all associated with the landing of Tropical Storm Dolly south of the Texas/Mexico border. Other large measurements were recorded during frontal passages.

Longshore current measurements are strongly correlated with local along shore winds measured at the collocated NWLON station, a 0.87 correlation for the alongshore currents measured by the offshore looking sensor. The correlation between alongshore wind and longshore currents measured by the nearshore looking sensor was not as strong at 0.73 with the difference attributed to the influence of the wave climate. The measured longshore current was also strongly correlated, 0.69, with further offshore currents measured by the TABS D buoy.

As current profilers are more difficult and expensive to maintain, a goal of the present work is to design and test nowcasting models predicting sensor readings based on other more permanent measurements collected in near real-time. A linear regression model was tested to predict significant wave height based on the standard deviation of the water levels measured at the collocated NWLON station. The model accuracy is presently characterized by a standard deviation of the residuals of 0.15 m. A more accurate model will likely be possible once more data is available and by optimizing the approach. A neural network approach was used to nowcast longshore currents based on along shore wind and the addition of other variables such as further offshore current measurements (TABS D), significant wave height and standard deviation of water levels. The accuracy of this preliminary nowcast model ranged between 0.100 m/s when including along shore wind only to 0.074 m/s when adding offshore longshore current and significant wave height to the model input.

Ongoing work includes continuing to measure nearshore conditions, designing and testing more accurate nowcasting models, comparing measurements with predictions from the NGOFS and NWPS (Near Shore Wave Prediction System) and further developing software to communicate the information to coastal stakeholders.

10. ACKNOWLEGEMENTS

Funding for the work presented in this paper is provided as part of a R&D 2014-2015 Funding Cycle grant from the Texas General Land Office (TGLO) and is gratefully acknowledged. The views expressed herein are those of the authors and do not necessarily reflect the views of TGLO.

The authors wish to acknowledge members of the Conrad Blucher Institute field crew and information technology teams for efficiently and creatively resolving problems throughout the project.

11. REFERENCES

Cox, D.T., P.E. Tissot, and P. R. Michaud, 2002a: Water Level Observations and Short-Term Predictions Including Meteorological Events for the Entrance of Galveston Bay, Texas. *J. of Wtwy, Port, Coast., and Oc. Engrg.*, 128-1, 21-29.

The MathWorks, Inc., 2014: *Neural Network Toolbox*, *Matlab R2014a*. The MathWorks, Natick, MA.

NDBC, cited 2015: Western Gulf of Mexico Recent Marine Data [Available online at http://www.ndbc.noaa.gov/maps/WestGulf.shtml.]

NOAA, cited 2015: Bob Hall Pier, Corpus Christi, TX – Station ID: 8775870 [Available online at

http://tidesandcurrents.noaa.gov/stationhome.html?id=8775870.]

NOAA, 1994: *NOAA Technical Memorandum NOS OES 8*. National Oceanic and Atmospheric Administration, Silver Spring, Maryland.

Park, J. R. Heitsenrether and W. Sweet, 2014: Water Level and Wave Height Estimates at NOAA Tide Stations from Acoustic and Microwave Sensors. *J. Atmos. Oceanic Technol.*, 31(10), 2294-2308, doi: 10.1175/JTECH-D-14-00021.1.

Parker, B., 1991: Tidal Hydrodynamics. Wiley, 912 pp.

Rizzo, J., P. Tissot and S. Duff (2014): The Texas Coastal Ocean Observation Network. *Proc. of Oceans' 14*, September 15-18, St. Johns, Newfoundland, CA. Institute of Electrical and Electronics Engineers, doi 10.1109/OCEANS.2014.7003131.

Simoniello, C., Tissot, P., McKee, D., Adams, A., Ball, R. and Butler, R. A., 2010: Cooperative Approach to Resource Management: Texas Gamefish Win. *J. Marine Technology Society*, vol.44(5), pp5-9, doi http://dx.doi.org/10.4031/MTSJ.44.5.5.

SonTek, 2009: Argonaut-SL System Manual Firmware Version 12.0. SonTek/YSI, San Diego, California, 316 pp. [Available online at ftp://rrcs-173-196-209-21.west.biz.rr.com/pub/outgoing/Argonaut-SL.pdf.]

Tissot, P.E., D.T. Cox, A. Sadovski, P. Michaud and S. Duff, 2004: Performance and Comparison of Water Level Forecasting Models for the Texas Ports and Waterways. *Proc. of the PORTS 2004 Conference*, Houston, TX, Amer. Soc. Civil Engineers [Available online at http://ascelibrary.org/doi/abs/10.1061/40727%282004%29129.]

Tissot, P.E., D.T. Cox, and P.R. Michaud, 2003: Optimization and Performance of a Neural Network Model Forecasting Water Levels for the Corpus Christi, Texas, Estuary. *Proc. of the 3rd Conference on the Applications of Artificial Intelligence to Environmental Science*, Long Beach, California, February 2003.

Wei, E., Z. Yang, Y. Chen, J.G.W. Kelley, A. Zhang (2014): The Northern Gulf Of Mexico Operational Forecast System (NGOFS): Model Development and Skill Assessment. NOAA Technical Report NOS CS 33, 190pp. [Available online at http://www.nauticalcharts.noaa.gov/csdl/publications/TR_NOS_CS33_FY_14_02_Eugene_NGOFS_report.pdf.]